

QUANTUM FLUCTUATIONS AND ELECTRONIC TRANSPORT THROUGH STRONGLY INTERACTING QUANTUM DOTS

T. A. COSTI (tac@tkm.physik.uni-karlsruhe.de)
*Universität Karlsruhe, Institut für Theorie der Kondensierten
Materie 76128 Karlsruhe, Germany*

Abstract. We study electronic transport through a strongly interacting quantum dot by using the finite temperature extension of Wilson's numerical renormalization group (NRG) method. This allows the linear conductance to be calculated at all temperatures and in particular at very low temperature where quantum fluctuations and the Kondo effect strongly modify the transport. The quantum dot investigated has one active level for transport and is modeled by an Anderson impurity model attached to left and right electron reservoirs. The predictions for the linear conductance are compared to available experimental data for quantum dots in heterostructures. The spin-resolved conductance is calculated as a function of gate voltage, temperature and magnetic field strength and the spin-filtering properties of quantum dots in a magnetic field are described.

1. Introduction

Recent experimental work [1–5] has demonstrated the importance of correlations in determining the low temperature transport properties of nanoscale size quantum dots. These dots consists of a confined region of electrons, of typical diameter 100nm , “weakly” coupled to leads via tunnel barriers. A “weak” coupling, Γ , means that the quantized levels of the dot are broadened into resonances, but are not completely washed out. A gate voltage, V_g , controls the position of the quantized levels relative to the chemical potentials of the leads and thereby the total number of electrons on the dot. The charging energy U for adding electrons to the dot from the surrounding electron reservoirs (leads) is typically the largest energy scale, and the dot is strongly correlated provided $U/\Gamma \gg 1$. Typical values for U and Γ for the dots in [1, 5] are $U \sim 0.5 - 2.0 \text{ meV}$ and $\Gamma \sim 0.2 - 0.3 \text{ meV}$, so these dots are strongly correlated.

For temperatures $\Gamma \ll T \ll U$ quantum fluctuations are small, and transport is dominated by charging effects. This regime is well understood [6]. The conductance, G , exhibits a series of approximately equidistant peaks as a function of V_g , with spacing U . The peaks correspond to a

fractional number of electrons on the dot and alternate “Coulomb blockade” valleys to either an even or an odd number of electrons.

In this paper we shall be interested in the regime $T \lesssim \Gamma \ll U$, where the strong quantum fluctuations can lead to a dramatic modification of the above picture of Coulomb blockade. In particular, for an odd number of electrons on the dot, the quantum dot can have a net spin 1/2, and a Kondo effect can develop. It has been predicted [7, 8], that, at low temperature, this enhances the conductance in the odd electron valleys, turning them instead into plateaus of near perfect transmission.

The outline of the paper is as follows. Sec. 2 describes the model and Sec. 3 the NRG method used to solve it. The results [9–11] for the conductance are described in Sec. 4–5 and these are used to compare with experiment over a range of gate voltages and temperatures in Sec. 6. Experimental investigation of the regime $T \lesssim \Gamma$ has only recently become possible as a result of better control of the electrode geometry, allowing parameters like Γ to be tuned to values of 1–3K so that $T \lesssim \Gamma$ is accessible [1–5]. Sec. 7 describes the effect of a magnetic field on the transport through a quantum dot. Influencing transport via spin effects is of great current interest [12]. The results presented in Sec. 7 should prove useful for interpreting magnetotransport experiments on strongly interacting quantum dots.

2. Model

At sufficiently low temperature, transport through a strongly interacting quantum dot will be mainly determined by the partially occupied level of the dot, denoted ε_d , which lies closest to the chemical potential of the leads. Its occupancy, n_d , can be varied from $n_d = 0$ to $n_d = 2$ by varying the gate voltage V_g , where $-eV_g = \varepsilon_d$. The resulting model of a single correlated level ε_d with Coulomb repulsion U , coupled to left and right free electron reservoirs can be written as

$$\begin{aligned} \mathcal{H} = & \sum_{\sigma} \varepsilon_d d_{\sigma}^{\dagger} d_{\sigma} + U d_{\uparrow}^{\dagger} d_{\uparrow} d_{\downarrow}^{\dagger} d_{\downarrow} + g \mu_B H S_z^d \\ & + \sum_{k,\sigma,i=L,R} \varepsilon_{k,i} c_{k,i,\sigma}^{\dagger} c_{k,i,\sigma} + \sum_{k,\sigma,i=L,R} V_i (c_{k,i,\sigma}^{\dagger} d_{\sigma} + d_{\sigma}^{\dagger} c_{k,i,\sigma}). \end{aligned} \quad (1)$$

We assume energy independent lead couplings $\Gamma_{L,R} = 2\pi\rho_{L,R}(\epsilon_F)V_{L,R}^2$, where $\rho_{L,R}(\epsilon_F)$ is the Fermi level density of states (per spin) of the left/right electron reservoir. The first two terms in \mathcal{H} represent the quantum dot, the third term is a magnetic field coupling only to the dot’s spin $S_z^d = \frac{1}{2}(d_{\uparrow}^{\dagger} d_{\uparrow} - d_{\downarrow}^{\dagger} d_{\downarrow})$ (we set $g = \mu_B = 1$), the fourth term represents the free electron reservoirs and the last term is the coupling between the dot and the reservoirs. This model can be reduced to the standard Anderson impurity

model of a single reservoir attached to the dot with strength $\Gamma = \Gamma_L + \Gamma_R$ [7]. Note that $\Gamma = 2\Delta$, where Δ is the hybridization strength as usually defined in the Anderson model [13]. We use Γ throughout. In experiments [1, 5], Γ is extracted by analyzing the high temperature ($T \gg \Gamma$) behaviour of the conductance peaks (see figure: 2a below).

We assume, from here on, symmetric coupling to the leads, $\Gamma_L = \Gamma_R$. The linear magnetoconductance, $G(T, H) = \sum_\sigma G_\sigma(T, H)$, is written as a sum of spin-resolved magnetoconductances, G_σ , where

$$G_\sigma(T, H) = \frac{e^2}{\hbar} \Gamma \int_{-\infty}^{+\infty} d\omega A_\sigma(\omega, T, H) \left(-\frac{\partial f(\omega)}{\partial \omega} \right). \quad (2)$$

$A_\sigma(\omega, T, H)$ is the equilibrium spectral density and is expressed in terms of the local level Green function, $\mathcal{G}_{d,\sigma} = 1/(\omega - \varepsilon_d + i\Gamma/2 - \Sigma_U)$, with Σ_U the correlation part of the self-energy, by

$$A_\sigma(\omega, T, H) = -\frac{1}{\pi} \text{Im} \mathcal{G}_{d,\sigma}(\omega + i\epsilon, T, H), \quad (3)$$

3. Method

We calculate $A_\sigma(\omega, T, H)$ by using Wilson's NRG method [14] extended to finite temperature dynamics [9, 15], with recent refinements [16, 17] which improve the high energy features. The NRG procedure for finite temperature dynamics is described in [9, 15]. Here, we make a few remarks concerning the above refinements.

The first refinement [16] uses the correlation part of the self-energy, Σ_U , to evaluate the spectral density A in the Anderson impurity model [16]. This improves the spectra around the single-particle excitations ε_d and $\varepsilon_d + U$ since the single particle broadening $\Gamma/2$ is put into the Green function, \mathcal{G}_d , exactly, thereby making the excitations at ε_d and $\varepsilon_d + U$ slightly sharper than in the earlier procedure [9] which evaluated A directly from its spectral representation. The description of the low energy Kondo resonance is equally accurate within both approaches and close to exact [16].

The second refinement uses the reduced density matrix in the NRG procedure for dynamical quantities [17] in place of the grand canonical density matrix of the usual procedure [9]. This reduces finite-size effects in the spectra. The latter are usually small on all energy scales in the case of zero magnetic field, but can be large in the case of a finite magnetic field, particularly for the high energy parts of the spectra (since these are calculated from the shortest chains and are therefore subject to the largest finite-size effects). Figure: 1a shows that both procedures give equally accurate results for the Kondo model in zero magnetic field on all energy

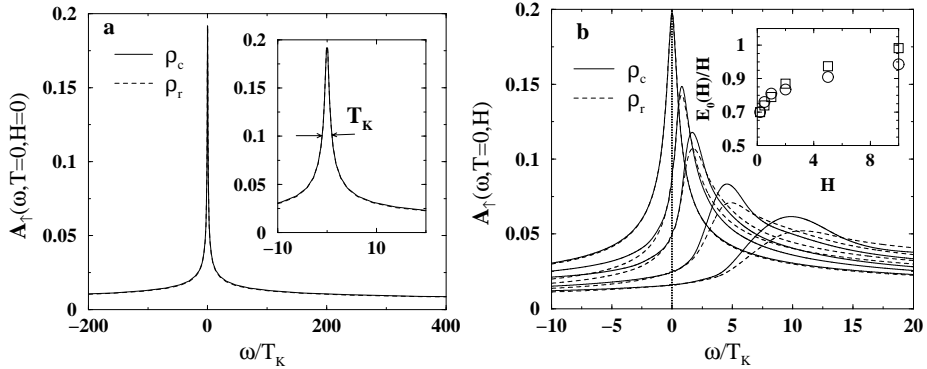


Figure 1. Comparison of methods for $A_>(\omega, 0, H)$, of the Kondo model, using canonical (ρ_c , solid line) [9] and reduced density matrices (ρ_r , dashed line) [17]. $T_K = 3.97 \times 10^{-5}$ (in units of half bandwidth $D = 1$) is the HWHM of the $T = H = 0$ Kondo resonance : (a) at zero field, with the inset showing the Kondo resonance in more detail, and, (b) in finite field, with the curves from left to right corresponding to $H = 0, 1, 2, 5, 10$ in units of T_K . The inset shows the peak position, $E_0(H)$, as a function of H for the canonical (circles) and reduced density matrix (squares) approaches. Both E_0 and H are measured in units of T_K . The limit [18] $\lim_{H \rightarrow 0} E_0(H)/H = 2/3$ is recovered in both approaches.

scales. The same holds for the Anderson model in zero magnetic field. At finite magnetic field, the reduced density matrix is required for a correct description of the features at ε_d and $\varepsilon_d + U$ in the spin-resolved spectra [17]. In contrast, the low energy Kondo resonance in a magnetic field is well described by either procedure for $H \lesssim 10T_K$, as shown in figure: 1b for the Kondo model.

The position, $E_0(H)$, of the spin-resolved Kondo resonance in a weak magnetic field, $H \ll T_K$, is known from an exact Fermi liquid result due to Logan [18] (see also [19] showing the low field quasiparticle resonance). This states that $\lim_{H \rightarrow 0} E_0(H)/H = 2/3$. This indicates that correlations reduce $E_0(H)/H$ from its expected high field limit of 1 to 2/3. The inset to figure: 1b shows that both procedures recover this result. The use of the reduced density matrix has also proven useful for studying magnetic states in the Hubbard model within the dynamical mean field theory [20].

4. Linear conductance for $H = 0$

The gate voltage dependence of the linear conductance of a quantum dot is shown in figure: 2a for a decreasing set of temperatures. There are three distinct physical regimes, corresponding to three ranges of the gate voltage controlling ε_d relative to the Fermi level (see also figure: 3a-c). In the empty (full) orbital regime (region 3) the conductance shows the expected activated behaviour as a function of temperature. In the mixed valent regime

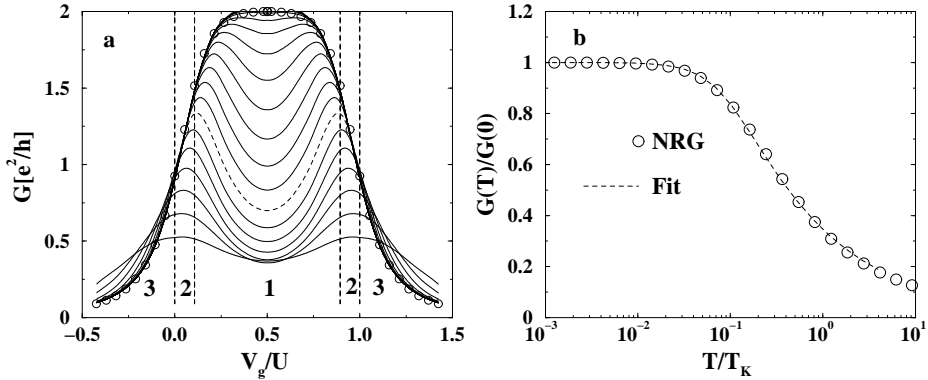


Figure 2. (a) $G(T, H = 0)$ versus V_g in the regime, $T \leq \Gamma$, of strong quantum fluctuations, for $U/\Gamma = 4.712$. The symbols are the $T = 0$ limit, Eq. (4). Temperatures decrease from bottom to top and correspond to $T_N = 0.64\Gamma\Lambda^{-N}$, $N = 0, 1, 2, \dots, \Lambda = 1.5$. The dashed curve has $T = 1.2T_K$, where $T_K \approx 0.05\Gamma$, is the HWHM of the $T = 0$ Kondo resonance at mid-valley gate voltage. The regions marked 1, 2 and 3 and separated by vertical dashed lines correspond to the Kondo ($\varepsilon_d \lesssim -0.5\Gamma$, i.e. $n_d \approx 1$), mixed valent ($|\varepsilon_d| \lesssim 0.5\Gamma$, i.e. $n_d \approx 0.5$, or by particle-hole symmetry, $|\varepsilon_d + U| \lesssim 0.5\Gamma$, i.e. $n_d \approx 1.5$), and empty (full) orbital regimes ($\varepsilon_d \gtrsim 0.5\Gamma$, i.e. $n_d \approx 0$, or, by particle-hole symmetry, $\varepsilon_d + U \lesssim -0.5\Gamma$, i.e. $n_d \approx 2$). (b) The universal conductance curve $G(T)/G(0)$ for a quantum dot in the Kondo regime at mid-valley, $V_g/U = 0.5$, (circles) [9, 10]. The dashed line is the fit formula $G(T)/G(0) = (T_K'^2/(T^2 + T_K'^2))^s$ with $s = 0.22$ and $T_K' = T_K/\sqrt{2^{1/s} - 1}$ used in [1] to interpolate the NRG results up to $10T_K$ (with T_K as in figure: 2a).

(region 2), the behaviour of G versus T is approximately that corresponding to tunneling through a resonant level close to the Fermi level. The most dramatic behaviour is in the Kondo regime (region 1), where one sees an anomalous enhancement of the conductance with decreasing temperature. The conductance continues to increase and eventually reaches the unitarity limit of $2e^2/h$ (see below) at mid-valley ($V_g/U = 0.5$ or $n_d = 1$). This remarkable enhancement of the conductance results from the formation, with decreasing temperature, of the many-body Kondo resonance at the Fermi level of the leads. The three types of behaviour have been observed in experiments on quantum dots carried out at $T \lesssim \Gamma$ [1, 5, 21]. The unitarity limit of the conductance, $2e^2/h$, has also recently been observed [5]. The $T \rightarrow 0$ conductance curve depends only on n_d via the Friedel sum rule [7, 8, 22]

$$G(T = 0, H = 0) = \frac{2e^2}{h} \sin^2(\pi n_d/2), \quad (4)$$

and is shown in figure: 2a (circles), with n_d deduced from the spectral densities as a check on the calculations.

5. Scaling of the linear conductance at $H = 0$

In the Kondo regime, $G(T)/G(0)$, is a universal function of T/T_K starting from low temperatures and extending up to some high temperature which depends on other details such as the precise value of Γ and ε_d . The latter energy scales cut off the universal behaviour of the conductance on the high temperature side. The universal conductance curves for the Kondo and Anderson models have been calculated for the experimentally interesting temperature range $0 \leq T \leq 10T_K$ via the NRG [9–11]. This is shown for the Kondo model in figure: 2b together with an approximate interpolating formula used in [1]. The scaling of $G(T)/G(0)$ with T/T_K shown in figure: 2b persists in the Anderson model throughout the Kondo regime (region 1) as long as $T \ll \Gamma$. At higher temperatures and in the other regimes, the conductance curves deviate from this universal shape (see Sec. 6 below). The Kondo scaling of the conductance in figure: 2b agrees well with measurements for both quantum dots in heterostructures [1, 5] and carbon nanotubes [21].

6. Comparison with experiment

For a comparison of theory with experiment in all regimes, the complete set of conductance curves for the Anderson model is required. These are shown in figure: 3a-c. $G(T)$ in the empty orbital and mixed valent regimes has been calculated in [23] and used to compare with experimental data in [1]. Here we make a parameter free comparison to similar data from Reference [5] for all three regimes of interest. The results are shown in figure: 3d. In making the comparisons, we estimated $G(T = 0)$ from $G(T = 30\text{mK})$, close to the lowest effective electron temperature $T = 40\text{mK}$ [5], and used it to determine n_d from Eq:4 and hence the appropriate ε_d to use in the NRG calculation for $G(T)$ at all T . The calculations also used the values of $\Gamma = 231.4\mu\text{eV}$ and $U \approx 0.5\text{meV}$ from the experiments. It is remarkable that this zero parameter comparison yields the agreement seen. The Kondo scale automatically comes out correctly as seen for the $V_g = -414\text{mV}$ comparison, and the agreement with the theoretical conductance curve is very good up to 700mK . The conductance curve used here includes the non-universal corrections discussed above and therefore differs slightly from that used in [5] (notably a slope change at 500mK due to corrections from charge fluctuations). The general trends of the experimental data in going to the mixed valent ($V_g = -420\text{mV}$, $V_g = -422\text{mV}$) and empty orbital cases ($V_g = -424\text{mV}$, $V_g = -426\text{mV}$) are well reproduced by the calculations. In particular the expected finite T peak in $G(T)$ [23] develops and becomes increasingly more pronounced on entering the empty orbital

regime. As described earlier, transport in this regime is likely to involve additional neighbouring levels and a larger conductance at higher temperatures, as observed in the experiments. In this light, the main discrepancy remaining between theory and experiment appears to be the dip in $G(T)$ at 200-300mK in the measurements. No signature of this is present in our model calculations. This could be due to interference effects associated with more than one level. It would therefore be interesting to investigate this possibility further.

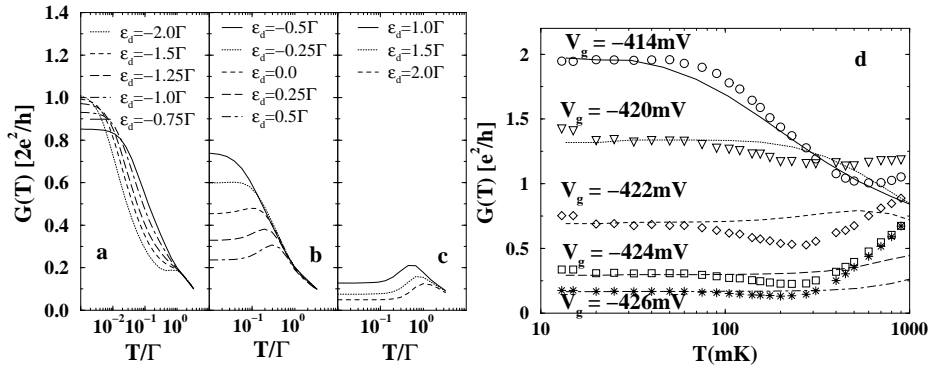


Figure 3. (a-c) $G(T)$ for gate voltages $V_g = -\varepsilon_d/e$ in, (a), the Kondo (K) regime, (b), the mixed valent (MV) regime ($\varepsilon_d = -0.5\Gamma, \dots, +0.5\Gamma$), and, (c), the empty orbital (EO) regime ($\varepsilon_d = +\Gamma, \dots, +2.0\Gamma$), and parameters as in figure: 2a. (d) Comparison of theoretical (lines) to experimental (symbols) conductance curves, $G(T)$, for the quantum dot in [5] with $U = 0.5\text{meV}$, $\Gamma = 0.231\text{meV}$ and $13\text{mK} \leq T \leq 900\text{mK}$. The values used for ε_d in the calculations were $\varepsilon_d = -0.85\Gamma$ ($V_g = -414\text{mV}$, K), $\varepsilon_d = -0.25\Gamma$ ($V_g = -420\text{mV}$, MV), $\varepsilon_d = +0.375\Gamma$ ($V_g = -422\text{mV}$, MV), $\varepsilon_d = +1.00\Gamma$ ($V_g = -424\text{mV}$, EO), $\varepsilon_d = +1.50\Gamma$ ($V_g = -426\text{mV}$, EO). We find a linear dependence $V_g/e = -\alpha\varepsilon_d$ for $V_g \leq -420\text{mV}$, which is a consistency check for determining ε_d from $G(T \rightarrow 0)$ using Eq. 4.

7. Effect of a magnetic field

A magnetic field suppresses the Kondo effect on a scale of T_K [13] and consequently it is expected to have a drastic effect on the conductance of a quantum dot [10, 11]. Indeed, figure: 4a shows that a field of $H = T_K$ suffices to reduce the $T = 0$ conductance at mid-valley to nearly half its value at $H = 0$ (cf. figure: 2a). This can be understood from the splitting of the Kondo resonance in a magnetic field and its strong reduction at the Fermi level (see figure: 1b and [10]). The suppression of the conductance is large in the whole Kondo regime (region 1) as long as $T \lesssim T_K$. At higher temperatures and in the other regimes, the effect of a field on the total conductance is less pronounced. However, in these regimes too, there can be a large effect in the *spin-resolved* conductances (see below).

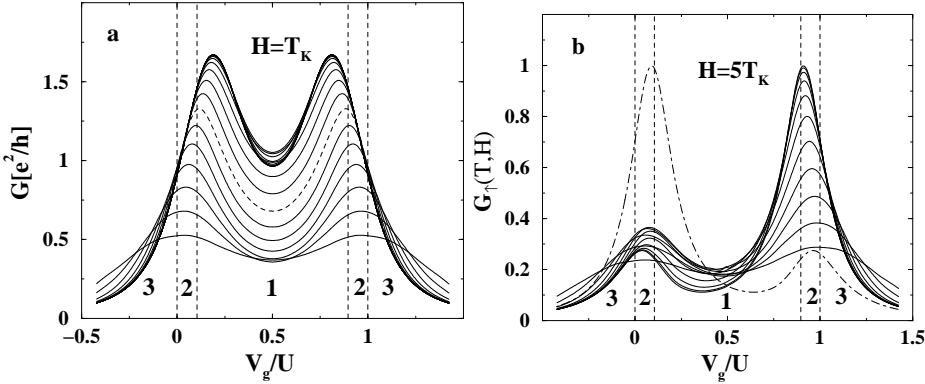


Figure 4. (a) T and V_g dependence of $G(T, H)$ for $H = T_K$ and for temperatures and parameters as in figure:2a. (b) T and V_g dependence of the spin-resolved conductance $G_\uparrow(T, H)$ for $H = 5T_K$ and for temperatures and parameters as in figure:2a. The dot-dashed curve is for the down spin conductance, $G_\downarrow(T, H)$, at the lowest temperature.

The effects of a magnetic field become even more apparent in spin-resolved quantities such as G_\uparrow in figure: 4b (by particle-hole symmetry G_\downarrow is the mirror reflection of G_\uparrow about $V_g/U = 0.5$). As in G , a magnetic field has a large effect on the spin-resolved conductance in the Kondo regime. In addition, there is quite a dramatic spin-filtering effect in the mixed valent regime, with $|G_\uparrow(0, H) - G_\downarrow(0, H)|$ being largest in this regime. In contrast, both up and down spin conductances are approximately equally suppressed in the other regimes. A quantum dot in a field is seen to act as a spin-filter as discussed in [24] for dots very weakly coupled to leads ($G_\sigma \ll e^2/h$).

The field dependence of the conductance of quantum dots defined in carbon nanotubes has been studied [21] and a preliminary comparison between our results and the experimental $G(B, T \lesssim T_K)$ shows good agreement [25].

8. Conclusions

We considered electronic transport through a strongly interacting quantum dot in zero and finite magnetic fields and in the low temperature regime $T \lesssim \Gamma$ where quantum fluctuations strongly modify the transport for an odd number of electrons on the dot.

The NRG conductance curves, $G(T, V_g)$, were used to make a parameter free comparison with experimental results of Reference [5] and we found good agreement. Discrepancies in the empty orbital regime where attributed to the neglect, within our model, of neighbouring levels

The results for the magnetoconductance in the Kondo regime exhibited the strong suppression of the Kondo effect by a magnetic field. A large spin-filtering effect was found in the mixed valent regime.

The field of non-equilibrium transport through quantum dots remains largely unexplored. Perturbative methods valid in the limit of large transport voltage, and magnetic field, $V, H \gg T_K$, are being developed [26], but non-perturbative techniques, such as extensions of NRG, will be required to address strong coupling.

Acknowledgements

I would like to thank the authors of Reference [5] for sending me the experimental data used in figure: 3b and W. van der Wiel for useful discussions. Financial support from the Deutsche Forschungsgemeinschaft, and in part by the National Science Foundation under Grant No. PHY99-07949 during the writing of this paper at the KITP of UCSB, is acknowledged.

References

1. D. Goldhaber-Gordon et al., *Phys. Rev. Lett.* **81**, 5225, 1998.
2. S. M. Cronenwett, T. H. Oosterkamp and L. Kouwenhoven, *Science* **281**, 540, 1998.
3. J. Schmid et al., *Physica B* **256**, 182, 1998.
4. F. Simmel et al., *Phys. Rev. Lett.* **83**, 804, 1999.
5. W. G. van der Wiel et al., *Science* **289**, 2105, 2000.
6. C. W. J. Beenakker and H. van Houten, *Solid State Physics*, **44**, 1 (1991).
7. L. I. Glazman and M. E. Raikh, *Sov. Phys. JETP Lett.* **47**, 454, 1988.
8. T. K. Ng and P. A. Lee, *Phys. Rev. Lett.* **61**, 1768, 1988.
9. T. A. Costi, A. C. Hewson and V. Zlatić, *J. Phys. Cond. Matt.* **6**, 2519, 1994.
10. T. A. Costi, *Phys. Rev. Lett.* **85**, 1504, 2000.
11. T. A. Costi, *Phys. Rev. B* **64**, 241310(R) 2001.
12. Y. Ohno et al., *Nature* **402**, 790, 1999.
13. A. C. Hewson, *The Kondo Problem to Heavy Fermions* (Cambridge University Press, Cambridge, England 1993)
14. K. G. Wilson, *Rev. Mod. Phys.* **47**, 773 (1975); H. R. Krishna-murthy, J. W. Wilkins and K. G. Wilson, *Phys. Rev. B* **21**, 1003, 1980.
15. T. A. Costi, in *Density Matrix Renormalization*, edited by I. Peschel, X. Wang, M. Kaulke and K. Hallberg (Springer, Berlin, Germany 1999).
16. R. Bulla, A. C. Hewson and Th. Pruschke, *J. Phys. Cond. Matt.* **10**, 8365, 1998.
17. W. Hofstetter, *Phys. Rev. Lett.* **85**, 1508, 2000.
18. D. E. Logan and N. L. Dickens, *J. Phys.: Condens. Matter* **13**, 9713, 2001.
19. A. C. Hewson, *J. Phys.: Condens. Matter*, **13**, 10011 (2001).
20. R. Zitzler, Th. Pruschke and R. Bulla, *European Phys. Journal*, **B27**, 473, 2002.
21. J. Nygård, D. H. Cobden and P. E. Lindelof, *Nature* **408**, 342, 2000.
22. D. C. Langreth, *Phys. Rev.* **150**, 516, 1966.
23. J. König and H. Schoeller, *Phys. Rev. Lett.* **84**, 3686 2000.
24. P. Recher, E. V. Sukhorukov and D. Loss, *Phys. Rev. Lett.* **85**, 1962, 2000.
25. J. Nygård, private communication.
26. A. Rosch, J. Paaske, J. Kroha, P. Wölfle, cond-mat/0202404.

